

Seeded epitaxy of $\text{Co}_{90}\text{Fe}_{10}/\text{Cu}$ multilayers on $\text{MgO}(001)$: Influence of Fe seed layer thickness

W. Kuch,^{a)} A. C. Marley, and S. S. P. Parkin

IBM Research Division, Almaden Research Center, 650 Harry Road, San Jose, California 95120

(Received 27 June 1997; accepted for publication 28 January 1998)

Epitaxial (001) $\text{Co}_{90}\text{Fe}_{10}/\text{Cu}$ multilayers were grown by sputter deposition on $\text{MgO}(001)$ substrates using bilayer seed layers containing thin Fe and Pt layers. The influence of the thickness of the Fe layer on the structure of the $\text{Co}_{90}\text{Fe}_{10}/\text{Cu}$ multilayers was studied by x-ray diffraction, and compared to its effect on the giant magnetoresistance measured in these films. The structural quality, especially of the $\text{Co}_{90}\text{Fe}_{10}/\text{Cu}$ layers closest to the seed bilayer, and the change in magnetoresistance depend sensitively on the Fe seed layer thickness. The largest giant magnetoresistance effect is found for Fe thicknesses around 12 Å. The influence of the Fe layer thickness is discussed in terms of lattice matching between the substrate, Fe, Pt, and $\text{Co}_{90}\text{Fe}_{10}/\text{Cu}$ layers, and alloying of Fe and Pt in the seed layer. © 1998 American Institute of Physics. [S0021-8979(98)03509-9]

INTRODUCTION

The controlled growth of magnetic multilayers on insulating substrates has become one of the most important issues in the application of giant magnetoresistance (GMR) for magnetic data storage head technology.¹ A system of particular interest is that of Co/Cu and related structures because this system exhibits the largest GMR effects at room temperature.² The magnetoresistive properties of this system depend strongly on the structural quality of the layered films.^{2–6} In polycrystalline Co/Cu multilayers grown on silicon it was discovered that a thin Fe seed layer approximately 50 Å thick gave greatly enhanced GMR values.² However, in order to explore the detailed relationship between structure and GMR, *single crystalline* films are most useful because this allows the detailed structure to be determined, for example, via x-ray scattering techniques. Because of the requirement of electrical non-conductivity, the choice of suitable substrates for growing such multilayers is limited. An appropriate means to accommodate the different lattice parameters of the substrate and the magnetic film is the use of seed layers, which are deposited onto the substrate prior to the growth of the magnetic multilayer. This seed layer has to mediate the lattice matching between the substrate and the multilayer, and to initiate an epitaxial relationship. Seed layers of several tens of Å of Pt, for example, have proven useful for growing (111) oriented epitaxial Co films on *c*-plane sapphire substrates.⁷

MgO is a commonly employed substrate for epitaxial growth of multilayers. The epitaxy of fcc transition metal ferromagnets ($a = 3.5\text{--}3.6$ Å), however, is hindered by a huge lattice mismatch (MgO : cubic NaCl structure, $a = 4.21$ Å). Pt, with an intermediate lattice spacing of 3.92 Å, is therefore a good candidate for the use as a seed layer. Epitaxial growth of Pt on $\text{MgO}(001)$ by magnetron sputtering

has been reported for substrate temperatures above 550 °C.⁸ Although the Pt is predominantly (001) oriented, the epitaxy is not perfect because of the simultaneous presence of a considerable amount of (111) oriented Pt. This can be reduced by further increasing the temperature, but even at 680 °C there still remains some (111) oriented material.⁸ The situation seems even worse when using molecular beam epitaxy to deposit Pt on $\text{MgO}(001)$ instead of plasma sputtering, because about half of the Pt assumes the (111) orientation at growth temperatures as high as 700 °C.⁹ To avoid the (111) orientation it has already been proposed to use Fe as a seed layer for the growth of Pt on $\text{MgO}(001)$. The initial sputter deposition of a few Å of Fe onto $\text{MgO}(001)$ prior to deposition of Pt yielded (001) epitaxial films with no (111) oriented material already at 350 °C.⁸

It seems obvious that the structural quality and hence the magnetic and magnetoresistive properties of magnetic multilayers depends strongly on the structure and morphology of the seed layers onto which they are deposited. Thus it is of interest to carry out a systematic study of the influence of the seed layer structure on, for example, GMR. To address this point, we present here structural and magnetoresistive properties of $\text{Co}_{90}\text{Fe}_{10}/\text{Cu}$ multilayers, grown on a combined seed layer consisting of sequentially deposited Fe and Pt layers on $\text{MgO}(001)$. The Fe thereby acts as the seed layer for the Pt seed layer. The structural properties of this two-step seed layer were systematically modified by varying the thickness of the initial Fe layer. Iron grows on $\text{MgO}(001)$ in the (001)-oriented bcc bulk phase with the in-plane [100] axis rotated by 45° with respect to the MgO substrate.¹⁰ The surface nearest neighbor distance of Fe of 2.87 Å thereby lies midway between those of Pt(001) (2.77 Å) and $\text{MgO}(001)$ (2.98 Å), respectively. It has been reported that the initial epitaxy of Fe on $\text{MgO}(001)$ proceeds by the growth of an islanded film with an intralayer lattice parameter very close to that of bulk bcc Fe. For increasing Fe layer thickness the lattice parameter monotonically increases up to 2.933 Å at about 8–10 monolayers (ML). For thicker films the Fe lattice

^{a)}On leave from (present address): Max-Planck-Institut für Mikrostrukturphysik, Weinberg 2, D-06120 Halle, Germany; Electronic mail: kuch@port.exp.bessy.de

constant decreases gradually to approach the bulk value in the thick film limit.¹⁰ It can thus be expected that varying the Fe seed layer thickness will have an influence on the subsequent growth of the Pt seed layer, and hence on the growth of the multilayer. We will show that there is indeed a systematic variation of the structural quality of the multilayers and the observed GMR on the Fe seed layer thickness, which should be taken into account when designing multilayers for high $\Delta R/R$ ratios.

For this investigation we used $\text{Co}_{90}\text{Fe}_{10}/\text{Cu}$ multilayers which exhibit rather large GMR effects and good structural quality.¹¹ $\text{Co}_{90}\text{Fe}_{10}$ and Cu are both fcc, with similar bulk lattice constants of 3.54 and 3.61 Å, respectively.¹² Because of this small lattice mismatch of less than 2% an epitaxial matching of the in-plane atomic distances within the multilayers is expected, and confirmed by our results.

EXPERIMENT

MgO(001) substrates of $2 \times 11 \text{ mm}^2$ size were cleaned by rinsing first in a buffered dilute solution of NH_4OH followed by rinsing in distilled water and drying in isopropyl alcohol vapor. The miscut of the MgO crystals was found to be less than 0.8° . The films were prepared by dc magnetron sputtering from high purity targets of iron, platinum, copper, and $\text{Co}_{90}\text{Fe}_{10}$. Typical sputter conditions were 0.4 Pa Argon and deposition rates of $\approx 2 \text{ Å/s}$. The Fe and Pt seed layers were grown at a substrate temperature of $\approx 770 \text{ K}$. Heating of the substrates was carried out by tantalum foil heaters. The temperatures reported here are those measured at the platter, and may be lower at the substrate holder. Before the deposition of the seed layers, the substrates were allowed $\approx 30 \text{ min}$ to thermalize in order to minimize the possibility of temperature drift during the deposition of a series of films. The samples presented here were prepared in two series, each of which consisted of 7 different structures on 7 MgO substrates. Reference samples, grown under identical conditions but without variation of the seed layer thickness showed no indication of an influence of a possible temperature drift on their structural properties. After allowing $\approx 200 \text{ min}$ for cooldown, the multilayers were deposited at $T \approx 315 \text{ K}$, and capped with 30 Å Pt to prevent oxidation. The sample structures are $\text{MgO}(001)/\text{Fe}(t_{\text{Fe}})/\text{Pt}(50 \text{ Å})/[\text{Co}_{90}\text{Fe}_{10}(10 \text{ Å})/\text{Cu}(9 \text{ Å})]_n/\text{Pt}(30 \text{ Å})$, where t_{Fe} was in the range between 2 and 14 Å, and $n = 6$ or 42. Layer thicknesses are those calibrated by mechanical profilometry of $\approx 1000 \text{ Å}$ reference films grown on quartz substrates. Deviations from the quoted thicknesses are less than 5%, and are limited by the stability of the sputter sources.

X-ray diffraction data were obtained under ambient pressure and temperature with a commercial four-circle diffractometer with monochromatized Cu $K\alpha$ radiation.

The magnetoresistance measurements were carried out using a standard four-point dc setup at room temperature, with magnetic field applied along the $\langle 100 \rangle$ or the $\langle 110 \rangle$ azimuth of the samples. The $\Delta R/R$ data were normalized to the resistance at 6 T field. The values reported in this paper correspond to the data for field applied along $\langle 110 \rangle$ with the current applied along $\langle 100 \rangle$. Several identical measurements

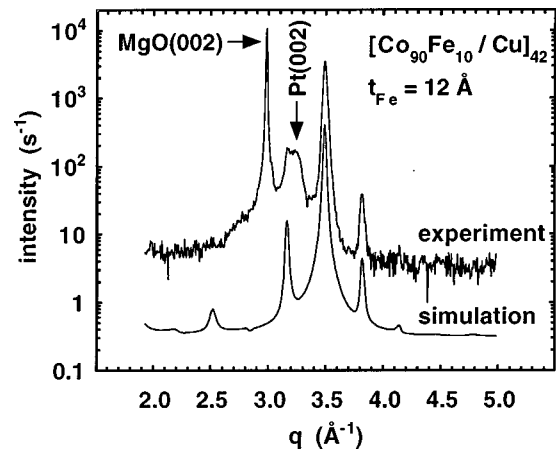


FIG. 1. Top: Specular $\Theta/2\Theta$ x-ray diffraction scans around the (002) diffraction of a $[\text{Co}_{90}\text{Fe}_{10}/\text{Cu}]_{42}$ multilayer, grown on a 12 Å Fe seed layer. (002) diffraction peaks of the Pt layers and the multilayer are indicated by arrows. Bottom: Simulation of $[\text{Co}_{90}\text{Fe}_{10}/\text{Cu}]_{42}$ specular scattering (see text).

were repeated on various samples to obtain an estimate of the experimental uncertainties. Excellent reproducibility was found.

RESULTS

The upper curve of Fig. 1 shows a specular $\Theta - 2\Theta$ scan of a $[\text{Co}_{90}\text{Fe}_{10}/\text{Cu}]_{42}$ multilayer, grown on a seed layer containing 12 Å of Fe. The sharp peak at a scattering vector of $q = 2.98 \text{ Å}^{-1}$ is the (002) diffraction of the MgO substrate, as indicated in the figure. The prominent peak at 3.49 Å^{-1} and two smaller peaks at $q = 3.17$ and 3.82 Å^{-1} (as well as a very small peak around 4.15 Å^{-1}) are attributed to (002) scattering from the $\text{Co}_{90}\text{Fe}_{10}/\text{Cu}$ multilayer. This splitting of the (002) diffraction is due to the periodicity of the multilayer, and demonstrates the high structural quality and sharp interfaces of the multilayered films. The lower curve shows a simulation of the specular diffraction of a free standing $[\text{Co}_{90}\text{Fe}_{10}/\text{Cu}]_{42}$ multilayer. The simulation was calculated using a computer code of Fullerton *et al.*¹³ The multilayer was modeled with identical lateral, but different vertical lattice spacings for the $\text{Co}_{90}\text{Fe}_{10}$ and the Cu layers. These were assumed to be constant over the entire stack. No strain profiles within the layers, and no interdiffusion was taken into account. The parameters for the simulation shown in Fig. 1 were obtained from fitting the diffraction data (upper curve) for $q > 3.4 \text{ Å}^{-1}$ to that model. This yielded atomic interlayer spacings of 1.76 Å for $\text{Co}_{90}\text{Fe}_{10}$, 1.83 Å for Cu, and a width of the continuous interface roughness¹³ of 0.09 Å. These layer spacings are consistent with laterally expanded $\text{Co}_{90}\text{Fe}_{10}$ layers, and compressed Cu layers. The peak separation of the satellite peaks corresponds to a periodicity of 19.2 Å, which is in excellent agreement with the layer thicknesses determined from the reference films.

From comparison of the experimental diffraction curve to the simulation, (002) scattering from the Pt in the seed and capping layers is easily identified at $q = 3.21 \text{ Å}^{-1}$, as indicated in Fig. 1. A contribution from seed layer Fe(002) scattering, which would be expected around 4.37 Å^{-1} , is not

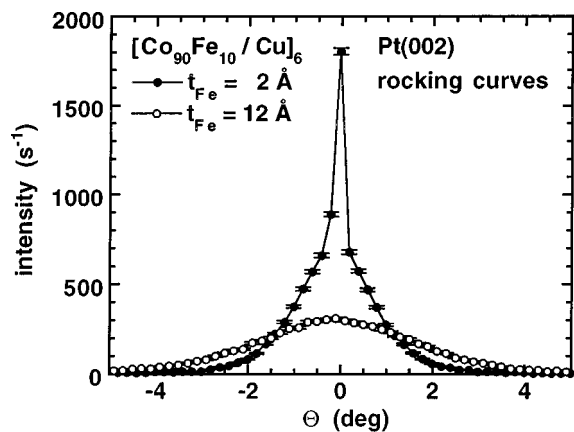


FIG. 2. Rocking curves of the specular Pt(002) diffraction of films grown on seed layers containing 2 Å (filled symbols) and 12 Å of Fe (open symbols).

detected within the noise level. This might be attributed to the small thickness of the Fe layers. No specular Pt(111) scattering could be detected in any of the films, suggesting the Pt layer is fully (001) oriented. Predepositing as little as 2 Å of Fe prior to Pt deposition thus appears to completely suppress the formation of (111)-oriented Pt, in line with the findings of Ref. 8

In-plane lattice constants of the multilayers, averaged over the entire thickness of the films, were calculated from the 2θ values of off-specular (111) and the specular (002) diffraction peaks. Values of 3.58 Å and 3.61 Å were found for the multilayers containing 42 and 6 repeats of $\text{Co}_{90}\text{Fe}_{10}/\text{Cu}$ respectively. The lower value of the thicker films indicates that there is tensile stress introduced by the substrate and the underlying seed layers (and perhaps also by the cap layer). The influence of this stress becomes less important at higher film thicknesses, resulting in a lattice relaxation towards smaller in-plane spacings. The measured in-plane lattice constants are independent of the Fe seed layer thickness for both the multilayers with $n=6$ and 42. This means that by changing the seed layer structural properties the multilayer lattice parameters are not strongly affected. In the following we will see that it is the quantity of structural imperfections in the multilayers which is mainly affected by the seed layer properties.

A simple measure of the structural quality of a thin film is the width of a rocking curve. Pt rocking curves have been taken at the maximum intensity of the specular Pt(002) diffraction. As seen from Fig. 1, Pt(002) scattering can be unambiguously separated from the satellite intensity of the multilayer (002) scattering. This holds especially for $n=6$ because of the lower satellite intensity compared to $n=42$. Figure 2 shows Pt rocking curves of a $[\text{Co}_{90}\text{Fe}_{10}/\text{Cu}]_6$ multilayer grown on seed layers containing 2 Å (filled symbols) and 12 Å of Fe (open symbols). For $t_{\text{Fe}}=2$ Å the rocking curve comprises two different contributions, namely a sharp peak with a full width at half maximum (FWHM) of less than 0.2° , superimposed on a broader peak with a width of 1.9° . Qualitatively identical Pt rocking curves were observed from samples with $[\text{Co}_{90}\text{Fe}_{10}/\text{Cu}]_{42}$ multilayers. The peak shape and overall width were reproducible to within $\pm 0.2^\circ$ for each sample. Similar rocking curves have also

been observed for Pt on *c*-plane sapphire.⁷ The sharp feature indicates the presence of a high degree of structural perfection in the Pt film grown on 2 Å of Fe. The broad component may arise from a distribution of structural defects present in the film. With increasing Fe seed layer thickness the intensity of the sharp peak is strongly decreased, and falls to zero for $t_{\text{Fe}} \geq 12$ Å (Fig. 2). The FWHM of the broader component increases from 1.9° at $t_{\text{Fe}}=2$ Å to 3.7° at $t_{\text{Fe}}=12$ Å. The number of structural imperfections in the Pt layers consequently shows a strong dependence on the thickness of the Fe seed layer, with less perfect Pt films on thicker Fe seed layers. Concomitantly the lattice parameters of the Pt layers change. The maximum of the Pt(002) specular diffraction peak shifts from 3.192 \AA^{-1} at $t_{\text{Fe}}=2$ Å continuously to 3.214 \AA^{-1} at $t_{\text{Fe}}=12$ Å. In thin films, interference fringes associated with the thickness of the film may cause small shifts in the position of Bragg peak maxima. However the Pt layers show rather broad peaks on a smooth background so that the 0.7% change in peak position may nevertheless be attributed to a 0.7% change in lattice spacing, such that for thicker Fe layers a smaller Pt lattice parameter is found. The same behavior is also observed for the off-specular Pt(111) diffraction. One has to keep in mind that the peaks reflect scattering from both the seed and capping layers. However, from the fact that a similar behavior of the Pt q values is observed for films containing either 6 or 42 bilayers of $\text{Co}_{90}\text{Fe}_{10}/\text{Cu}$, we conclude that the change in peak position is mostly due to changes in the seed layer.

A compilation of the results of measurements of the specular (002) rocking curve width of Pt and the multilayer is presented in the lower part of Fig. 3. The four lowermost curves show the FWHM of the broad component of the Pt(002) rocking curves (circles), and of the multilayer rocking curves (squares), plotted versus the Fe seed layer thickness for both the case of 6 repeats (open symbols), and 42 repeats (filled symbols) of $\text{Co}_{90}\text{Fe}_{10}/\text{Cu}$ in the multilayer. The error bars were obtained from multiple measurements of the same sample, and represent the accuracy of determining the rocking curve widths. The above mentioned dependence on t_{Fe} of the Pt rocking curve width is easily seen. The small differences between $n=6$ and $n=42$ at higher Fe thicknesses must be attributed to contributions from the cap layer, since the films were grown under identical conditions, and the seed layers as well as the first repeats of the multilayer should thus be identical. The rocking curve width of the $[\text{Co}_{90}\text{Fe}_{10}/\text{Cu}]_6$ multilayer is about constant around 5.8° up to $t_{\text{Fe}}=6$ Å, and decreases to reach 4.8° at $t_{\text{Fe}}=12$ Å. These high FWHM values indicate a high degree of structural disorder in the first 6 bilayers of the multilayer. The structural disorder in the initial layers of the multilayer is partly improved by increasing the Fe seed layer thickness to 12 Å. For $n=42$ much lower values are observed, ranging from 1.72° at $t_{\text{Fe}}=4$ Å to 1.50° at $t_{\text{Fe}}=12$ Å. The same tendency of decreasing rocking curve width for increasing Fe seed layer thickness is observed for both $n=42$ and $n=6$, although it is less pronounced for $n=42$. From this and the above mentioned differences in the overall in-plane multilayer lattice constant (3.61 vs 3.58 Å) we conclude that the multilayer at the initial stages of epitaxy is strained towards higher in-

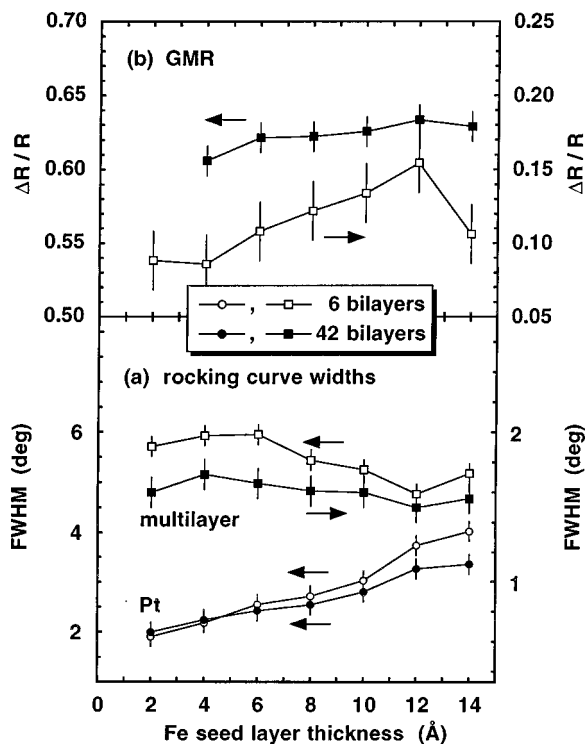


FIG. 3. Structural and magnetoresistive properties of multilayer samples containing 6 bilayers (open symbols) and 42 bilayers (filled symbols) of $\text{Co}_{90}\text{Fe}_{10}/\text{Cu}$ as a function of Fe seed layer thickness. (a) FWHMs of the specular (002) rocking curves of the multilayer (squares), and of the Pt layers (circles). (b) $\Delta R/R$ ratio at room temperature. Note the different scales for the rocking curve width of the multilayer for $n=42$, and the $\Delta R/R$ data for $n=6$.

plane lattice constants, and relaxes towards smaller values at higher thicknesses. Since the multilayer lattice constant does not change when varying the Fe seed layer thickness, the different degree of structural disorder in the multilayer consequently must be introduced by the different lattice mismatch between the multilayer and seed layer. The mechanisms which enable the fast accommodation of this considerable mismatch may result in structural imperfections such as local deformation of lattice planes and mosaic spread, being more pronounced for a larger mismatch. It is interesting that the dependence of Pt and multilayer rocking curve width on the Fe seed layer thickness have opposite trends: the more imperfections and defects are present in the Pt layer, the more perfect is the growth of the multilayer on top of this Pt layer. Structural defects as a consequence of seed layer structural defects can therefore be ruled out.

In the upper part of Fig. 3 the corresponding $\Delta R/R$ ratios at room temperature are shown for the multilayers with 6 bilayers (open symbols) and 42 bilayers (filled symbols) of $\text{Co}_{90}\text{Fe}_{10}/\text{Cu}$. The dependence on the Fe seed layer thickness, although clearly seen in both cases, is much more pronounced for $n=6$. This corresponds with the dependence of the multilayer rocking curve width on t_{Fe} being more pronounced for $n=6$. In that case, but also for $n=42$, a clear one to one correlation between the GMR and the structural quality of the multilayers, as judged from the rocking curve FWHM, can be stated. Maximum $\Delta R/R$ ratios (and minimum FWHMs) are obtained at 12 Å Fe layer thickness, with

values of 15.4% and 63.3% for 6 and 42 bilayers of $\text{Co}_{90}\text{Fe}_{10}/\text{Cu}$, respectively. The optimum procedure to grow $\text{Co}_{90}\text{Fe}_{10}/\text{Cu}$ multilayers by seeded epitaxy on $\text{MgO}(001)$ thus would be to predeposit 12 Å of Fe prior to the deposition of the Pt seed layer.

DISCUSSION

As mentioned before, the number of imperfections present in the multilayer is not simply introduced by a more imperfect seed layer, since the opposite behavior is observed. One possible explanation may arise from the fact that with increasing thickness of the Fe seed layer on $\text{MgO}(001)$, the Fe in-plane lattice parameter is increased, as reported in Ref. 10. The maximum increase amounts to about 1.9%.¹⁰ The mismatch between Fe and Pt is accordingly significantly enhanced from 3.5% up to 5.6%. In addition, the initial growth of Fe on $\text{MgO}(001)$ proceeds by the formation of separated Fe islands.¹⁰ The larger number of structural imperfections in the Pt layer, which manifests itself in the observed higher FWHM of the Pt rocking curves, has then to be a consequence of depositing Pt on top of these Fe islands exhibiting coverage-dependent in-plane lattice spacings. It is conceivable that the higher roughness of the Fe-covered MgO surface, and the higher stress imposed on the Pt layer by the enhanced Fe lattice parameter in the Fe islands lead to the observed increase in FWHM of the Pt diffraction peak. Interestingly it is the less perfect structure of the Pt seed layer which leads to a higher structural perfection of the multilayers, especially in the initial layers, and to a higher GMR. The larger disorder in the Pt layer could have an impact on the mechanisms which accommodate the lattice mismatch to the Pt seed layer in the initial stages of growth of the $[\text{Co}_{90}\text{Fe}_{10}/\text{Cu}]$ multilayers. A less perfect crystalline structure of the Pt layer may lead to a less coherent growth, or to a more rapid reduction of the imposed stress in the multilayer, which in turn may account for the higher structural quality.

An alternate explanation is the possibility of intermixing between Fe and Pt in the seed layers which might lead to the formation of an FePt alloy. Deposition of Pt on the islanded Fe film at 770 K might be sufficient to form an FePt alloy, with the composition being a function of the amount of predeposited Fe. It has been published that annealing Pt/Fe multilayers for 14 h at 750 K¹⁴ as well as thermal coevaporation of Fe and Pt at 770 K¹⁵ leads to the formation of ordered FePt alloy films. We therefore do not want to exclude the possibility that in the Pt/Fe seed layers, which were deposited at 770 K, there might be already some interdiffusion and alloy formation between Fe and Pt. This could explain the x-ray diffraction data from the Pt layers, which indicate a 0.7% decrease in the average lattice spacing with increasing Fe seed layer thickness in both the Pt (002) and (111) crystalline directions. The higher amount of structural imperfection in the Pt layer could be a consequence of intermixing or doping with Fe. The less perfect structure, and also the different lattice parameter of the (Fe-)Pt seed layer may impose less stress on the multilayer, which in turn may lead to higher structural perfection.

On increasing t_{Fe} from 12 to 14 Å the films show an opposite trend with regard to the multilayer FWHM (and the GMR) than found for smaller Fe seed layer thicknesses. For $n=6$ the multilayer FWHM again goes up from 4.8° at $t_{\text{Fe}}=12$ Å to 5.2° at $t_{\text{Fe}}=14$ Å. The GMR is strongly affected, and drops from 15.4% to 10.6%. This decrease in GMR and increase in FWHM of the $\text{Co}_{90}\text{Fe}_{10}/\text{Cu}$ multilayers is statistically significant in the sense that it is larger than the experimental uncertainty of the FWHM and $\Delta R/R$ determination. However, it is not immediately clear whether this could not be due to some other experimental artifact, e.g., in the substrate preparation. It is, on the other hand, also observed in the multilayers containing 42 repeats of $\text{Co}_{90}\text{Fe}_{10}/\text{Cu}$ although less pronounced. These were grown in a separate series, so that the probability that the same artifact could be erratically reproduced in both series is low. We therefore cautiously attribute the reversed trend above 12 Å Fe seed layer thickness to an intrinsic property of the system. It could possibly be explained by the growth of Fe on $\text{MgO}(001)$. According to Ref. 10 the Fe lattice constant increases with thickness in the initial stages of growth, but decreases beyond approximately 8–10 ML. A minimum in the $\text{Fe}(110)$ diffraction peak width was observed around 8 ML.¹⁰ This was interpreted by Fe forming islands on the $\text{MgO}(001)$ surface in the initial stages of growth, and partially coalescing around 10 ML. Since 10 ML correspond to about 14 Å, it is conceivable that the onset of coalescence leads to the observed minima of the multilayer FWHM at $t_{\text{Fe}}=12$ Å. A partly coalesced Fe film may offer a smoother surface for the growing Pt film than Fe islands, which in line with the above interpretation leads to the reversed trend with increasing Fe thickness. Considering possible alloy formation, it is conceivable that some of the coalesced Fe material is not incorporated into the Pt layer, which would lead to a lower “effective” Fe layer thickness when alloying into the Pt layer is concerned. The question remains why this reversed trend is not also observed in the Pt FWHM, which then should decrease when going from 12 to 14 Å Fe layer thickness. Such a decrease may, however, be masked by the contribution of the Pt capping layer. As already mentioned, this contribution to the Pt scattering is thought to be responsible for the difference in the Pt rocking curve width between $n=6$ and $n=42$, which is largest at $t_{\text{Fe}}=14$ Å (Fig. 3).

In these studies we have used $\text{Co}_{90}\text{Fe}_{10}/\text{Cu}$ multilayers as a model system to systematically study the influence of the seed layer on their structural and magnetoresistive properties. In view of the similar atomic nearest neighbor distances of 3d metals, the effect of the Fe seed layer thickness will most probably be very similar in fcc multilayers composed of other 3d metals. The influence of the seed layer on multilayer properties is clearly more important for smaller

number of bilayers. When aiming at high $\Delta R/R$ ratios in structures with only a small number of bilayers, for example in spin valves, it can be of the utmost importance to carefully optimize the seed layer.

CONCLUSIONS

In summary, we have used a combined seed layer consisting of sequentially deposited Fe and Pt layers to epitaxially grow (001) $\text{Co}_{90}\text{Fe}_{10}/\text{Cu}$ multilayers. We have systematically varied the Fe seed layer thickness, and studied the structural and magnetoresistive properties of the multilayers. The influence of the seed layer becomes more pronounced for thinner multilayers. The best results with respect to both structural perfection and high $\Delta R/R$ ratios were obtained for an Fe seed layer thickness of 12 Å. We interpret the differences in multilayer properties introduced by varying the Fe seed layer thickness as due to changes of the morphology and the lattice parameter of the predeposited Fe, possibly in conjunction with an intermixing or alloying between the Fe and Pt in the seed layer.

ACKNOWLEDGMENTS

The authors thank M. F. Toney for helpful discussions, and K. P. Roche for his technical expertise. S.S.P.P. thanks the Office of Naval Research for partial support of this work.

- ¹S. S. P. Parkin, *Ultrathin Magnetic Structures II*, edited by B. Heinrich and J. A. C. Bland (Springer, Berlin, 1994).
- ²S. S. P. Parkin, Z. G. Li, and D. J. Smith, *Appl. Phys. Lett.* **58**, 2710 (1991).
- ³M. Suzuki, Y. Taga, A. Goto, and H. Yasuoka, *J. Magn. Magn. Mater.* **126**, 495 (1993).
- ⁴K. Kagawa, H. Kano, A. Okabe, A. Suzuki, and K. Hayashi, *J. Appl. Phys.* **75**, 6540 (1994).
- ⁵J. Xu, B. J. Hickey, M. A. Howson, D. Greig, M. J. Walker, and N. Wiser, *J. Magn. Magn. Mater.* **156**, 69 (1996).
- ⁶T. Kingetsu and F. Yoshizaki, *Jpn. J. Appl. Phys., Part 2* **33**, L854 (1994).
- ⁷R. F. C. Farrow, G. R. Harp, R. F. Marks, T. A. Rabedeau, M. F. Toney, D. Weller, and S. S. P. Parkin, *J. Cryst. Growth* **133**, 47 (1993).
- ⁸B. M. Lairson, M. R. Visokay, R. Sinclair, S. Hagstrom, and B. M. Clemens, *Appl. Phys. Lett.* **61**, 1390 (1992).
- ⁹P. C. McIntyre, C. J. Maggiore, and M. Nastasi, *J. Appl. Phys.* **77**, 6201 (1995).
- ¹⁰B. M. Lairson, A. P. Payne, S. Brennan, N. M. Rensing, B. J. Daniels, and B. M. Clemens, *J. Appl. Phys.* **78**, 4449 (1995).
- ¹¹Y. Saito, S. Hashimoto, and K. Inomata, *Appl. Phys. Lett.* **60**, 2436 (1992).
- ¹²W. B. Pearson, *A Handbook of Lattice Spacings and Structures of Metals and Alloys* (Pergamon, Oxford, 1958).
- ¹³E. E. Fullerton, I. K. Schuller, H. Vanderstraeten, and Y. Bruynseraede, *Phys. Rev. B* **45**, 9292 (1992).
- ¹⁴M. R. Visokay, B. M. Lairson, B. M. Clemens, and R. Sinclair, *J. Magn. Magn. Mater.* **126**, 136 (1993); B. M. Lairson, M. R. Visokay, R. Sinclair, and B. M. Clemens, *ibid.* **126**, 577 (1993).
- ¹⁵A. Cebollada, D. Weller, J. Sticht, G. R. Harp, R. F. C. Farrow, R. F. Marks, R. Savoy, and J. C. Scott, *Phys. Rev. B* **50**, 3419 (1994).